Thermal and mechanical properties of PP/HDPE/wood powder and MAPP/HDPE/ wood powder polymer blend composites

D.G. Dikobe[1,2], A.S. Luyt[3]*

[1] Department of Chemistry, University of the Free State (Qwaqwa Campus), Private Bag X13, Phuthaditjhaba, 9866, South Africa

[2] Department of Chemistry, University of Pretoria, Private Bag X20, Hatfield 0028, South Africa

[3] Center for Advanced Materials, Qatar University, PO Box 2713, Doha, Qatar

* Corresponding author (aluyt@qu.edu.qa)

Highlights

• Replacing PP with MAPP in 50/50 w/w blend composites with different amounts of wood powder (WP).

• Separation between PP and MAPP crystallization more resolved with increasing WP content.

• Cooling rate had a stronger influence on MAPP than on PP crystallization in the presence of WP.

•Replacement of PP with MAPP in the blend composites had an appreciable influence on the tensile properties.

Abstract

The morphology and properties of blends of PP/HDPE and MAPP/HDPE blends, and their composites with wood powder, were investigated in this paper. The blends showed two-phase morphologies, and MAPP interacted better than PP with HDPE, while the WP interacted more strongly with MAPP. Although the different components in the blends were immiscible, they showed one crystallization peak. MAPP and HDPE showed separate crystallization peaks in the composites, and this separation of the crystallization became more resolved with increasing WP content and at lower cooling rates. This was also observed for PP and HDPE

in their composites, but to a lesser extent. Young's modulus increased and the stress at break decreased with increasing WP content, and these were more pronounced in the PP/HDPE/WP composites. Interaction between WP and MAPP also had an influence on elongation at break. The presence of WP increased the thermal stability of the MAPP/HDPE and PP/HDPE.

Keywords: PP/HDPE; MAPP/HDPE; wood powder; composites; thermal properties; mechanical properties

1. Introduction

The demand for polymers with new properties can be met by blending two or more existing polymers. High-density polyethylene (HDPE) and propylene (PP) are abundant, cheap and can be easily processed; as a result, the binary blends of PP and HDPE have been investigated by a number of researchers [1-7]. HDPE has a low temperature impact resistance while PP has low impact strength. Theoretically, blends of PP and HDPE should provide blends with improved impact strength. However, due to the difference between the melting temperatures of PP and HDPE, blending of the two polymers results in immiscible blends with poor physical and mechanical properties [6-13]. For this reason, a compatibilizer is often used to promote compatibility between the two polymers [8].

Another method of improving the properties of polymers is by adding inorganic fillers such as clay, $CaCO_3$ and carbon black to form polymer composites [9]. Natural fibres are also used as polymer fillers due to their properties such as low density, biodegradability, recyclability and their abundance [10-12]. Most polymers are incompatible with natural fillers, and compatibilizers such as maleated PP (MAPP) are used to promote interfacial adhesion between the polymer and natural fillers, resulting in polymer composites with better properties [8,13,14].

New materials can also be developed by mixing two polymers and one filler. For this ternary system, addition of a suitable compatibilizer is still essential. The presence of maleated polyethylene (MAPE) or MAPP in a PP/HDPE/clay blend composite significantly improved the mechanical properties [15,16]. The interactions between the filler particles and the two polymers in the blend may result in three different morphologies depending on the affinity towards the polymers. The filler may disperse in one polymer, or in both polymers, or

at the interface between the two polymers [17]. The selective distribution of the fillers has an effect on the crystallization behaviour and other properties of ternary composites [18].

The addition of the fillers to a polymer increases the polymer's crystallization temperature due to the filler's nucleating ability [19]. The crystallization temperature also depends on the structure and crystallization rate of the polymer [20]. Carbon nanotubes [21,22], nanoclay [23,24] and wood powder [25] were found to have no influence on HDPE crystallization behaviour, but a reasonable increase in crystallization temperature was reported when fillers were added to PP [25]. At high cooling rates, PP/HDPE blends and PP/HDPE/clay composites showed similar crystallization behaviour, resulting in one broad exothermic peak [15,26]. Decreasing the cooling rate to 1 °C min^{-1} resulted in two separate crystallization peaks. The higher temperature exotherm was associated with the crystallization of PP due to the nucleation effect of clay, while the other exothermic peak (still in its original position) was associated with HDPE crystallization.

In most studies where MAPP was used, it was used in small amounts and as a compatibilizer. Our interest was to explore the possibility of using MAPP as a significant part of the polymer matrix, and comparing the properties of these blends and composites with those of composites with the same compositions, but where PP was used instead of MAPP. Wood powder was chosen as natural fibre filler because of its easy processing and environmental friendliness. To our knowledge there are only a few reports on similar systems [27-30].

The current study focused on a comparison of the properties of PP/HDPE and MAPP/HDPE blends, and on the composites formed when these blends were mixed with different amounts of wood powder (WP). Of special interest in this study was the influence of cooling rate on the crystallization and thermal behaviour of these blends and composites.

2. Materials and methods

2.1 Materials

Maleic anhydride grafted polypropylene (MAPP), supplied by Pluss Polymers Pvt. Ltd. (India), has a density of 0.91 g cm^{-3}, a melting point of 161 °C, a tensile strength of 24 MPa and a melt flow index (MFI) of 55 g/10min (190 °C, 2.16 kg). Polypropylene (PP), supplied by Sasol Polymers (Johannesburg, South Africa), has a density of 0.90 g cm^{-3}, a melting point

of 165 °C, and an MFI of 12 g/10min (230 °C, 2.16 kg). HDPE, supplied by Sasol Polymers (Johannesburg, South Africa), has a density of 0.956 g cm^{-3}, a melting point of 136 °C, and an MFI of 2.0 g/10 min (190 °C, 5 kg). Pine wood powder (WP), or pine saw dust, was obtained from FBW Taurus (Phuthaditjhaba, South Africa). WP was supplied as a light orange coloured powder with a density of 1.5 g cm^{-3}, and was dried at 120 °C for 48 hours. Particles with sizes ≤ 150 µm were obtained by sieving the dried WP using a laboratory test sieve of 150 µm pore size.

2.2 Preparation of blends and composites

The blends and blend composites were weighed according to the required ratios (50/50/0, 45/45/10, 40/40/20, 35/35/30 w/w PP/HDPE/WP and MAPP/HDPE/WP) to make up a total of 38 g (which is the mass required to thoroughly mix the different components in the Brabender Plastograph 50 mL internal mixer). Mixing of the samples was done at 180 °C and a mixing speed of 30 rpm for 15 minutes. The samples that were used for analysis were melt pressed at 190 °C and 100 bar for 3 minutes to form 1.5 mm thick sheets. The pressed samples were allowed to cool at room temperature for 10 minutes to avoid air from penetrating, which would promote the formation of bubbles. The neat polymers were treated in the same way.

2.3 Blends and composites analysis

The morphologies of the blends and the 40/40/20 w/w PP/HDPE/WP and 40/40/20 w/w MAPP/HDPE/WP blend composites were examined using a Shimadzu SSX-550 Superscan scanning electron microscope (SEM) (Bangkok, Thailand). The samples were immersed in liquid nitrogen before fracture, and the fractured surface was sputter coated with gold dust (60 nm) before viewing.

Fourier-transform infrared (FTIR) analyses were performed on the samples by using a Perkin Elmer Spectrum 100 FTIR spectrometer over a 400–4000 cm^{-1} wavenumber range at a resolution of 4 cm^{-1}.

Differential scanning calorimetry (DSC) analyses were carried out in a Perkin Elmer DSC7 differential scanning calorimeter under flowing nitrogen (20 mL min^{-1}). Two methods were used. In the first method, samples with masses of approximately 7.5 mg were heated

from 25 to 190 °C at a rate of 10°C min^{-1} to eliminate the thermal history, cooled to 25 °C at 10 °C min^{-1}, and reheated under the same conditions. The second method was the same as the first method, except that cooling was done at 2 °C min^{-1}. Three different samples were analyzed for each composition, and the melting and crystallization data were obtained from the second scan. The average values and standard deviations of these values are reported.

Tensile testing was performed under ambient conditions on a Hounsfield H5KS universal tester at a cross-head speed of 50 mm min^{-1}. The tensile test specimens (gauge length 24 mm, width 5 mm, thickness 2 mm) were prepared using a dumbbell shaped hollow punch. Six samples per composition were analysed, and the average and standard deviation values are reported.

Thermogravimetric analyses (TGA) were carried out using a Perkin Elmer TGA7 (Waltham, Massachusetts, USA). Samples with masses of approximately 10 mg were heated from 50 to 600 °C at a heating rate of 20 °C min^{-1} under flowing nitrogen (20 mL min^{-1}).

3. Results and discussion

3.1 Scanning electron microscopy (SEM)

The surface morphology of the samples was investigated through scanning electron microscopy (SEM) in order to relate the mechanical behaviour of the different blends and composites to their mechanical properties. The SEM images of the 50/50 w/w PP/HDPE blend, the 50/50 w/w MAPP/HDPE blend, and their composites with 20 wt.% WP are presented in Figure 1. Chiu *et al*. [16] observed two-phased morphology for the 50/50 w/w PP/HDPE blend. They reported that HDPE has a higher viscosity than PP and therefore HDPE was the dispersed phase and PP the continuous phase. However, Na *et al*. [31] observed elongated domains in the SEM images of 50/50 w/w PP/HDPE blends, and Clemmons [32] reported a co-continuous morphology in the 50/50 w/w PP/HDPE uncompatibilized blend, where the more ductile HDPE phase could be clearly distinguished from the PP phase. Although Figure 1(a) does not conclusively show the two phases, it looks (from the different shades of grey) as if this blend in our case has a co-continuous morphology, similar to the morphology described by Na *et al.* and Clemmons. Salih *et al*. [33] reported an interfacial adhesion between the dispersed domains and continuous phases in

an 80/20 w/w PP/HDPE blend, which could be the reason why we did not clearly distinguish the two phases in Figure 1(a).

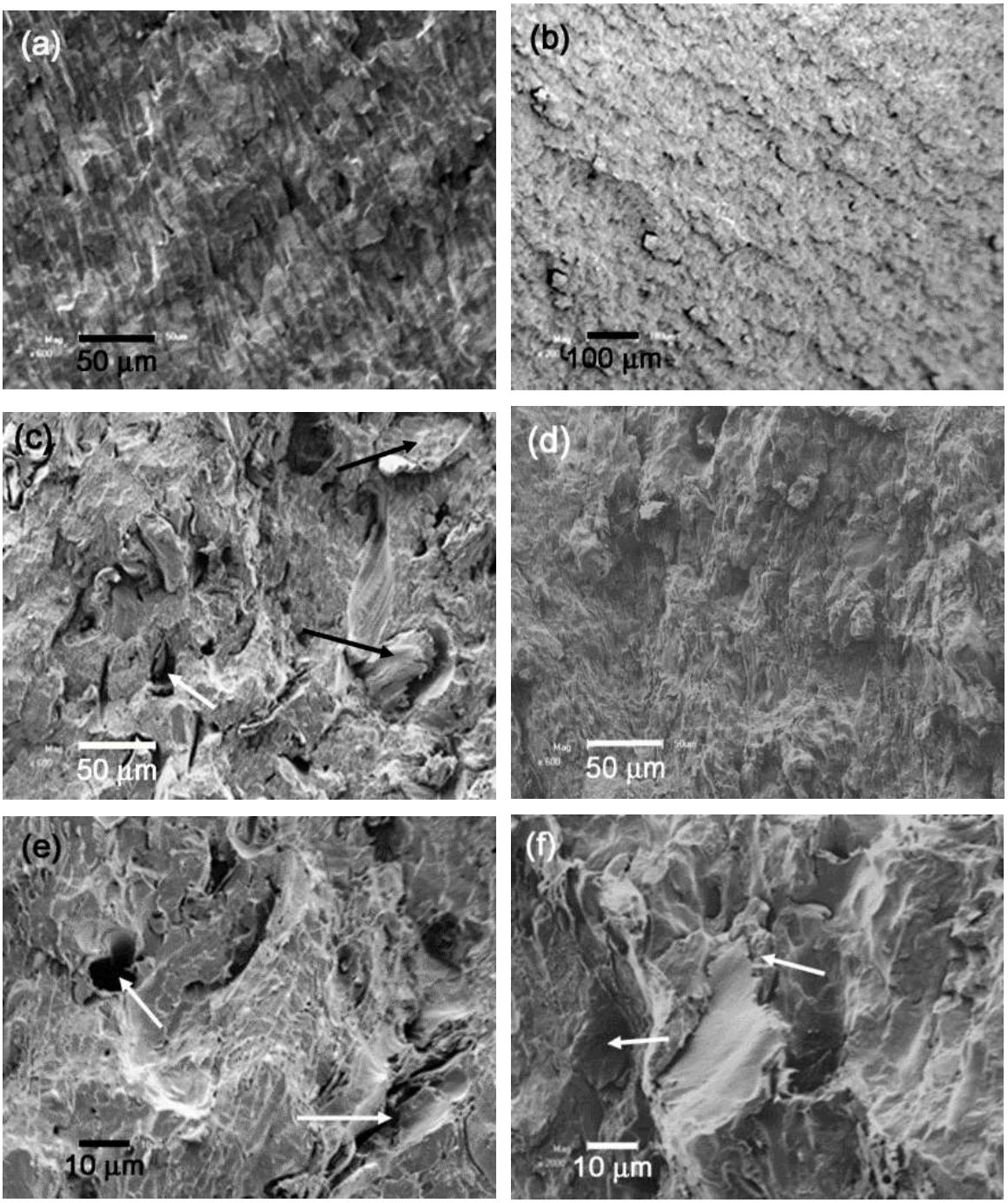

Figure 1 SEM images of the fractured surfaces of (a) 50/50 w/w PP/HDPE (600x), (b) 50/50 w/w MAPP/HDPE (200x), (c) 40/40/20 w/w PP/HDPE/WP (600x), (d) 40/40/20 w/w MAPP/HDPE/WP (600x), (e) 40/40/20 w/w PP/HDPE/WP (2000x), and (f) 40/40/20 w/w PP/HDPE/WP (2000x)

The SEM images of the 40/40/20 w/w PP/HDPE/WP at 600x and 2000x magnifications are presented in Figures 1(c) and 1(e). There are fibre pull-outs and cracks around the WP particles in both images (see arrows), indicating that there was poor compatibility between the

hydrophobic PP and HDPE, and the hydrophilic WP in the absence of a compatibilizer. Figures 1(d) and 1(f) clearly show a much more intimate contact between the polymer matrix and the WP particles (see arrows). The WP particles were probably surrounded by MAPP, with strong hydrogen bonding between the –OH groups of the WP cellulose and the anhydride groups on MAPP.

3.2 Fourier-transform infrared (FTIR) spectroscopy

FTIR spectroscopy was used to confirm possible interactions between the different components in the blends and composites. All the FTIR spectra in Figure 2 have strong absorbance peaks around 2850 and 2910 cm^{-1} associated with the -CH asymmetric stretching in the polymers. The PP and MAPP spectra have a -CH stretch around 2960 cm^{-1}, which is not present in the HDPE spectrum. This is due to the different ratios of CH_2 to CH_3 groups in the different polymers. The difference between the PP (Figure 2(a)) and MAPP (Figure 2(b)) spectra is that the MAPP spectrum has a characteristic absorption peak at 1740 cm^{-1} due to the symmetric -C=O stretching in the anhydride groups [34-37].

Changes in the FTIR spectra of the blends and the composites may indicate a possible reaction or interaction taking place the two polymers and between the polymers and the filler. The spectra in Figure 2(a) show peaks for HDPE at 720 and 1740 cm^{-1}. The peak at 720 cm^{-1} is due to the -CH_2 rocking vibrations, but the peak at 1740 cm^{-1} is normally associated with carbonyl groups and is not characteristic for HDPE. A possible explanation for this peak is the presence of an antioxidant in the commercially supplied HDPE. The PP spectrum shows an absorption around 1370 cm^{-1} and 3000 cm^{-1} due to -CH_3 symmetric and asymmetric medium stretch vibrations. The HDPE and PP absorption peaks at 1460 cm^{-1} are assigned to the scissor modes of the-C-H stretching. The PP/HDPE blend spectrum has the all the peaks observed for neat PP and HDPE. There is no appearance, disappearance or shifting of the peaks in this spectrum, confirming the absence of any interaction between these two polymers. This is reasonable, as no interaction or reaction is expected between PP and HDPE.

The MAPP spectrum in Figure 2(b) has absorption peaks at 2960, 2920 and 1470 cm^{-1} due to the asymmetric, symmetric and scissor modes of the –CH stretching. It also has a characteristic absorption peak at 1740 cm^{-1} due to the symmetric -C=O stretching in the anhydride groups. The MAPP spectrum also shows an absorption at 1370 cm^{-1} due to the -CH_3 vibrations. In the spectrum of the MAPP/HDPE blend the carbonyl peak has almost

disappeared, which could have been the result of a reaction between the functional groups on MAPP and the antioxidant in HDPE. Such a reaction could negatively influence the interaction between MAPP and WP in the blend composites.

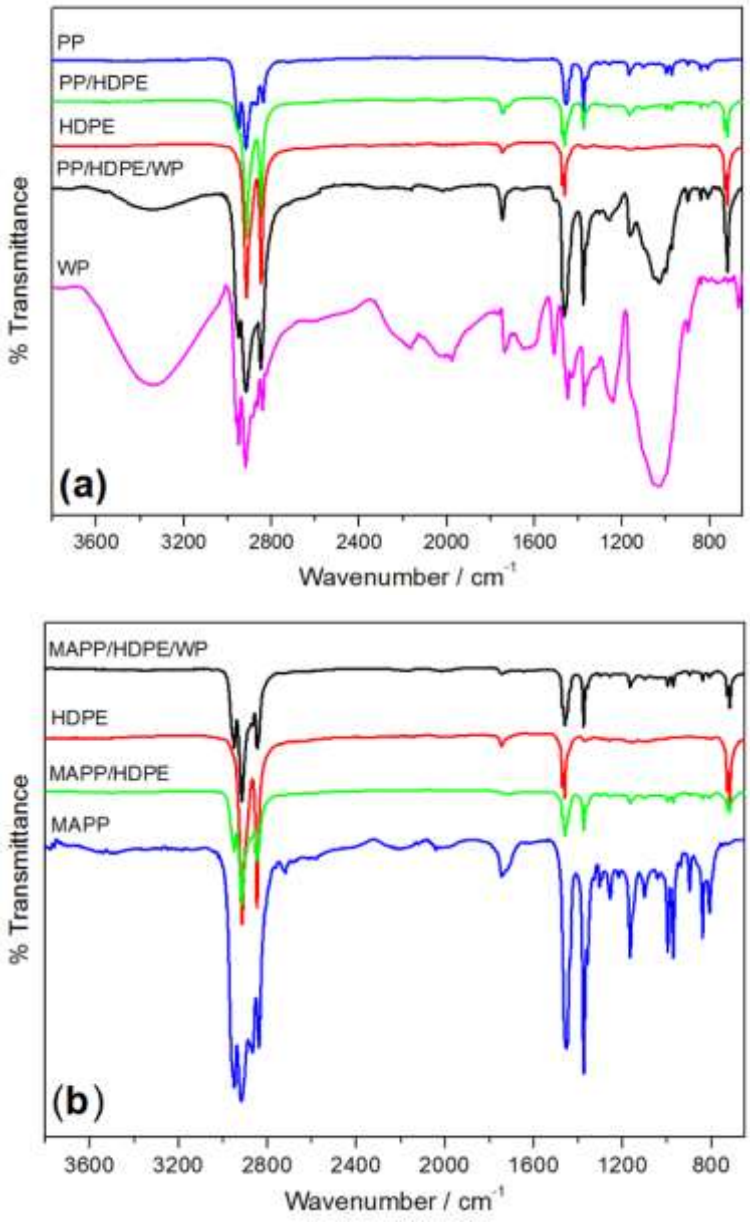

Figure 2 FTIR spectra of the (a) PP/HDPE/WP and (b) MAPP/HDPE/WP systems

The most important peak in the WP spectrum (Figure 2(a)) is a strong, broad –OH stretching vibration in the range of 3300-3500 cm^{-1}. The peak at 2910 cm^{-1} is due to -C-H stretching vibrations, while the peak at 1735 cm^{-1} is assigned to the -C=O unconjugated stretching of the carboxylic acid or ester of the hemicelluloses. The band at 1600 cm^{-1} is the –OH bending vibration. The peak around 1045 cm^{-1} is assigned to the –C-O stretching vibration of the acyl group present in the lignin [32,35].

The PP/HDPE/WP composite spectrum shows the peaks corresponding to the cellulosic filler. The –C=O group stretch slightly shifted from 1735 to 1745 cm^{-1} in the composite, while the $–CH_3$ stretch vibrations at 2960 and 1380 cm^{-1} for PP shifted to 2945 and 1360 cm^{-1} respectively in the blend composite. The positions of the characteristic peaks for PP remained the same in this spectrum. The observed shifts could be an indication of weak Van der Waals interactions between PP and WP.

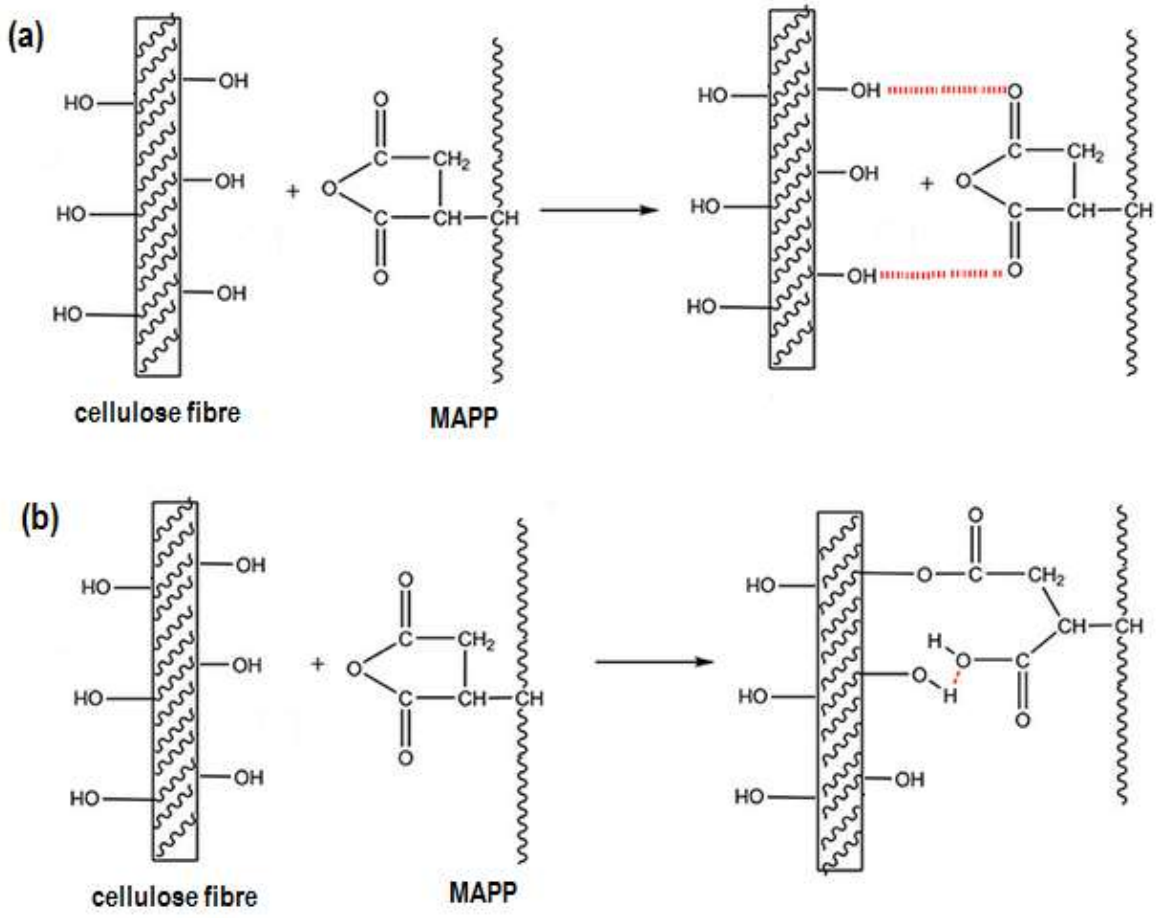

Figure 3 Schematic representation of possible mechanisms showing (a) interaction between MAPP and WP, and (b) reaction between MAPP and WP

In the FTIR spectrum of the MAPP/HDPE/WP composite, the MAPP carbonyl stretch has shifted from 1725 to 1716 cm^{-1} in the composite. The $–CH_3$ stretch vibrations at 2960 and 1370 cm^{-1} in MAPP shifted to 2935 and 1350 cm^{-1} in the blend composite, while the HDPE peaks were in the same positions as in the blend spectrum. The carbonyl peak around 1725 cm^{-1} is very weak in both the MAPP/HDPE and MAPP/HDPE/WP spectra, and it is difficult to establish changes in the peak position and intensity that may point to an reaction/interaction between the functional groups in MAPP and WP, although a strong hydrogen bonding

interaction is at least expected between the oxygen of maleic anhydride the carbonyl group and the hydrogen of the cellulose hydroxyl group [38], see Figure 3(a). The peak at 1045 cm^{-1}, assigned to the -C-O stretching vibration of the acyl group in the lignin, is missing in the MAPP/HDPE/WP spectrum due to a possible reaction between the cellulose and the anhydride ring (Figure 3(b)). This is a well-established reaction [39-41] and the final products are an ester and reactive groups from carboxylic acids. The intensity of the hydroxyl and the acetyl bands is strongly reduced as the carboxylic acid groups increase due to the primary -OH oxidation and/or the hydrolysis of acetyl groups from the hemicellulose. The –OH band reduction at 3400 cm^{-1} is also important as it shows the decrease in the polarity of lignin as the maleate or carbonyl groups replace the hydroxyl groups (Figure 3(b)). The appearance of the peak at 1740 cm^{-1} in the MAPP/HDPE/WP spectrum compared to that of the MAPP/HDPE blend indicates the presence of the carbonyl groups.

3.3 Differential scanning calorimetry (DSC)

3.3.1 Crystallization and melting behaviour of the neat polymers

The DSC cooling curves of the neat polymers at 2 and 10 °C min^{-1} are presented in Figure 4(a), and the heating curves after cooling at these rates are presented in Figure 4(b). The crystallization and melting temperatures and melting enthalpies, as well as the respective polymer's degrees of crystallinity (calculated by using Equation 1), are summarized in Tables 1 and 2.

$$\chi_c = (H_m^{exp} / wH_m^o) \times 100\% \qquad (1)$$

where H_m^{exp} is the melting enthalpy obtained from the area under the melting peak of the polymer, H_m^o is the melting enthalpy for a 100% crystalline polymer (208.8 J g^{-1} for PP and MAPP, and 288.8 J g^{-1} for HDPE [5]), and *w* is the weight fraction of each polymer in the blends and composites.

It is interesting that PP and MAPP crystallizes at almost the same temperature as HDPE, despite the relatively large difference in the melting temperature of HDPE, and those of PP and MAPP. The degree of supercooling (ΔT) is defined as the difference between the melting peak temperature (T_m) and the crystallization peak temperature (T_c) [19]. ΔT for PP and

MAPP is approximately 53 °C, whereas that of HDPE is 24 °C. ΔT is proportional to the free energy of melting which is the driving force of nucleation. The large ΔT values for PP and MAPP indicate that it will take longer before MAPP and PP nucleate during dynamic cooling. The simple, linear structure of the HDPE chain is highly flexible above its glass transition temperature, and will therefore crystallize more easily than PP and MAPP with the $–CH_3$ and other functional side groups. HDPE crystallizes more rapidly with less supercooling than PP and MAPP, which is the reason for the overlap in crystallization peaks of the two polymers in the respective blends.

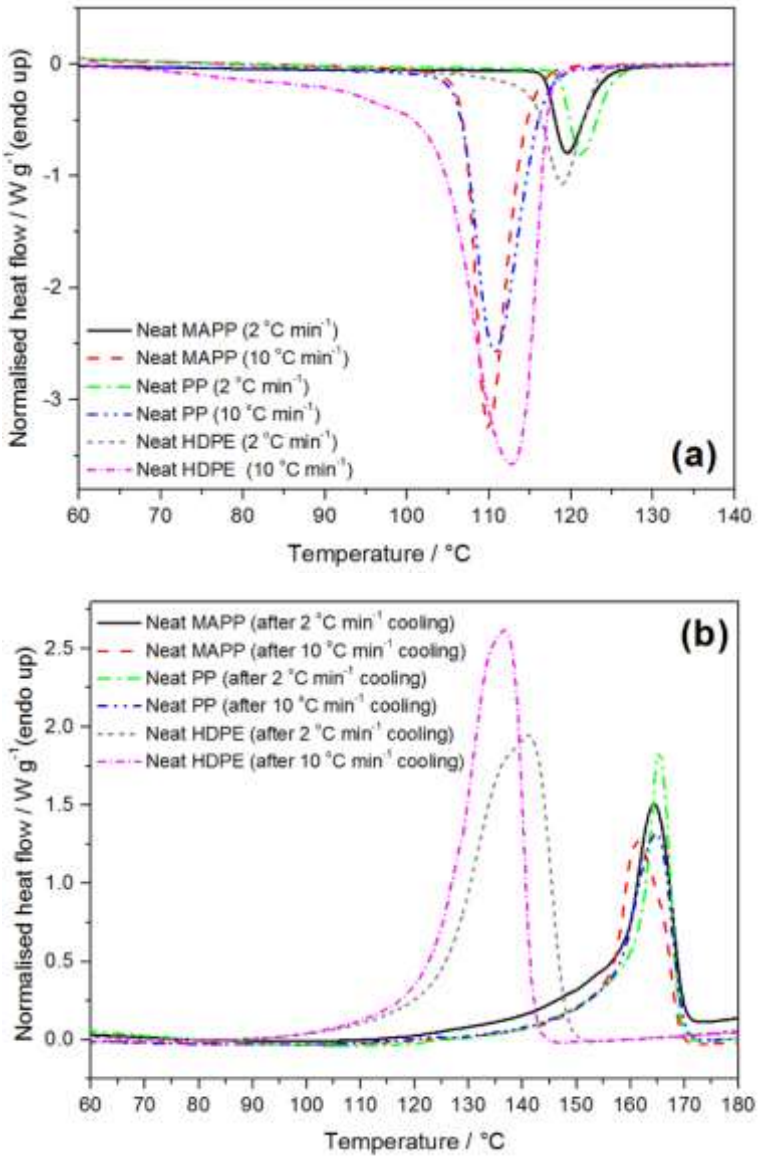

Figure 4 DSC (a) cooling and (b) heating curves of the neat polymers

Since the DSC is normally more sensitive at faster cooling/heating rates, and since all three polymers are known to have relatively fast crystallization rates, all the crystallization

peaks are more well-defined for a cooling rate of 10 °C min^{-1}. If one looks at the crystallization peak temperatures for HDPE, PP and MAPP at the two cooling rates, one observes that HDPE crystallized at a lower temperature than PP and MAPP when the cooling rate was low, but at a higher temperature when the cooling rate was higher. This is because HDPE has a lower steric hindrance to crystallization than PP and MAPP. It has been reported that polymers with symmetrical and short repeating chain segments crystallize faster than those with longer, unsymmetrical or branched repeating units [20].

It is, however, interesting to see that the HDPE cooled at 10 °C min^{-1} shows a sharper, more well-defined melting peak with a lower-temperature peak maximum than the sample cooled at 2 °C min^{-1} (Figure 4(b)), indicating smaller crystallites with a narrower size distribution. Its total crystallinity also seems to be higher when cooled at a faster rate (Table 1). This has previously been explained through secondary crystallization during faster cooling [19]. Secondary crystallization occurs when there may be inadequate time for complete spherulite development during the primary crystallization phase. Additional polymer chains continue to move onto existing crystals and crystallization continues beyond the primary phase, although at a slower rate. This results in a further increase in crystallinity after primary crystallization [19]. An increase in the X_c of HDPE during fast cooling can be attributed to secondary crystallization (see Table 1 and 2) as compared to slow cooling which is dominated by primary nucleation.

Although there are small differences in the shapes and sizes of the PP and MAPP melting peaks after cooling at the two different rates, the total crystallinity and crystal size distribution (as evidenced from the peak widths in Figure 3(b), and the melting temperature and crystallinity data in Tables 1 and 2) did not change as significantly as in the case of HDPE. A lower temperature 'tail' before the melting at 165 °C is observed when PP and MAPP were heated after cooling at both 10 and 2 °C min^{-1}. PP generally consists of a mixture of the α- and β-crystal phases [42]. The β-crystals and the small imperfect α-crystals normally melt in the 140-160°C temperature range, while the α-crystals melt at about 165°C [42]. The observed PP and MAPP melting peaks are probably the result of an overlap of these two melting events.

3.3.2 Crystallization and melting behaviour of the blends

The cooling curves of the PP/HDPE and MAPP/HDPE blends at the two cooling rates are presented in Figure 5(a). In both blends the crystallization peaks of the two polymers overlap. Finlay *et al.* [43] studied slow cooled PP/HDPE blends and reported that the crystallization curves of iPP and HDPE overlap, making it difficult to resolve the two components. Lin *et al.* [1] reported that the crystallization peaks of PP and HDPE cannot be distinguished from each other due to the quick crystallization of HDPE. The blending of PP and HDPE apparently accelerates the heterogeneous nucleation of PP. For both cooling rates, once the HDPE nucleus is formed in the molten blends, the PP and MAPP molecules have the same mobility to enter the crystals and form a co-crystal morphology. For both cooling rates, there was a small decrease in the crystallinity of HDPE, but a fairly significant decrease in those of PP and MAPP (Tables 1 and 2). This is probably because HDPE will homonucleates first, followed by the heteronucleation of MAPP and PP on HDPE. The HDPE crystals probably impedes the mobility of the PP and MAPP chains, making it more difficult for the chains to arrange themselves into an ordered crystalline structure. Slow cooling of both blends resulted in an increase in the crystallization temperatures, because there is sufficient time for the heteronucleation process to start at higher temperatures.

The heating curves of the PP/HDPE and MAPP/HDPE blends cooled at different rates are shown in Figure 5(b). The blends, at both cooling rates, show two well resolved endothermic melting peaks corresponding to those of the PP or MAPP and HDPE phases. This confirms the immiscibility of the two polymers. The melting temperatures of HDPE, PP and MAPP in the blends did not significantly change from those of the neat polymers after cooling at 10 °C min^{-1}. However, after cooling the blends at 2 °C min^{-1}, the HDPE melting temperature decreased from 141 °C for the neat polymer to 136 °C for HDPE cooled in the presence of PP and MAPP. At the faster cooling rate, because HDPE crystallizes faster than PP or MAPP, the HDPE crystals had time to grow before transcrystallization of the PP or MAPP on the HDPE crystals. At the slower cooling rate heteronucleation took place and the HDPE crystal growth was impeded by the presence of PP or MAPP crystals. The smaller HDPE crystals gave rise to a lower melting temperature.

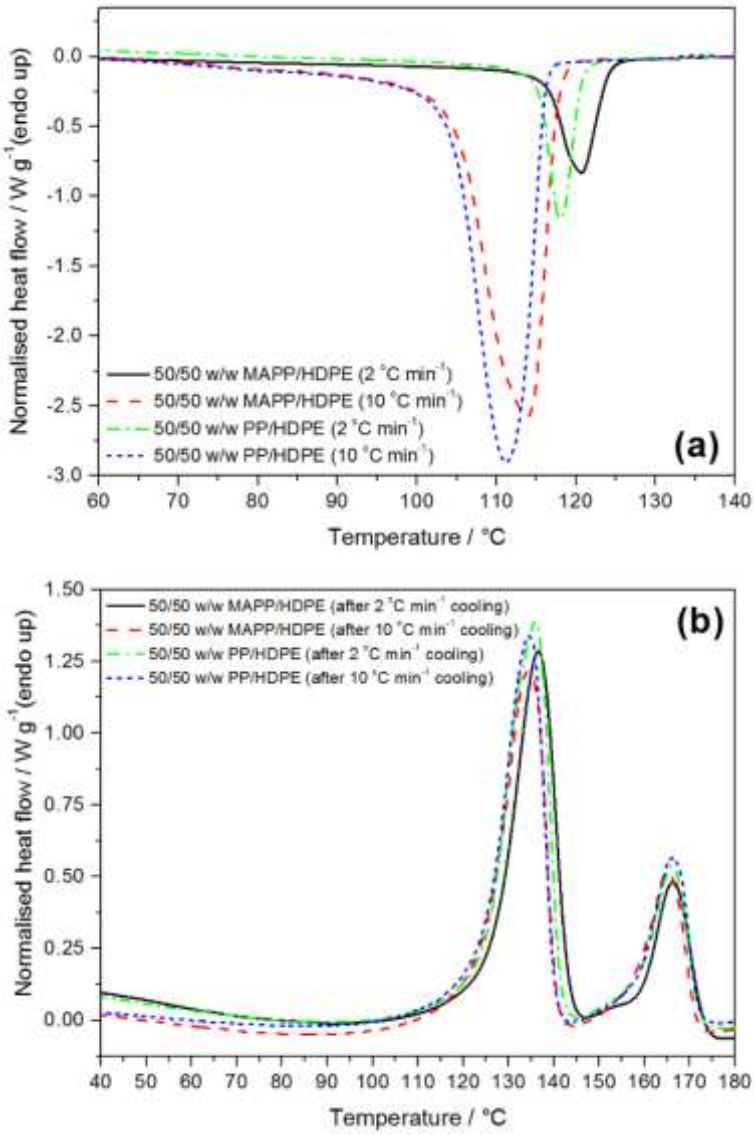

Figure 5 **DSC (a) cooling and (b) heating curves of the blends**

3.3.3 Crystallization and melting behaviour of the blend composites

The cooling and re-heating curves of the blend composites with 20 and 30 % WP are presented in Figure 6. The first observation from Figure 6 (and Tables 1 and 2) is (i) that cooling at 2 °C min^{-1} gave rise to two crystallization peaks for both PP/HDPE/WP and MAPP/HDPE/WP, (ii) that the two peaks were more resolved for MAPP/HDPE/WP, (iii) that they became even more resolved at the higher WP contents; and (iv) that cooling at 10 °C min^{-1} gave rise to two peaks only for MAPP/HDPE/WP, and that the peaks are also more resolved at higher WP contents. Because of its preferential nucleation of PP and MAPP, the WP particles caused PP and MAPP to start crystallizing at higher temperatures, while they

had little influence on the HDPE crystallization, with the MAPP crystallizing at higher temperatures than the PP under the same analysis conditions because the WP obviously interacted more strongly with the MAPP. This stronger interaction with MAPP caused a separation of the crystallization peaks even at a higher cooling rate, while the interaction with PP was not strong enough to cause the PP to crystallize separately at 10 °C min^{-1} cooling.

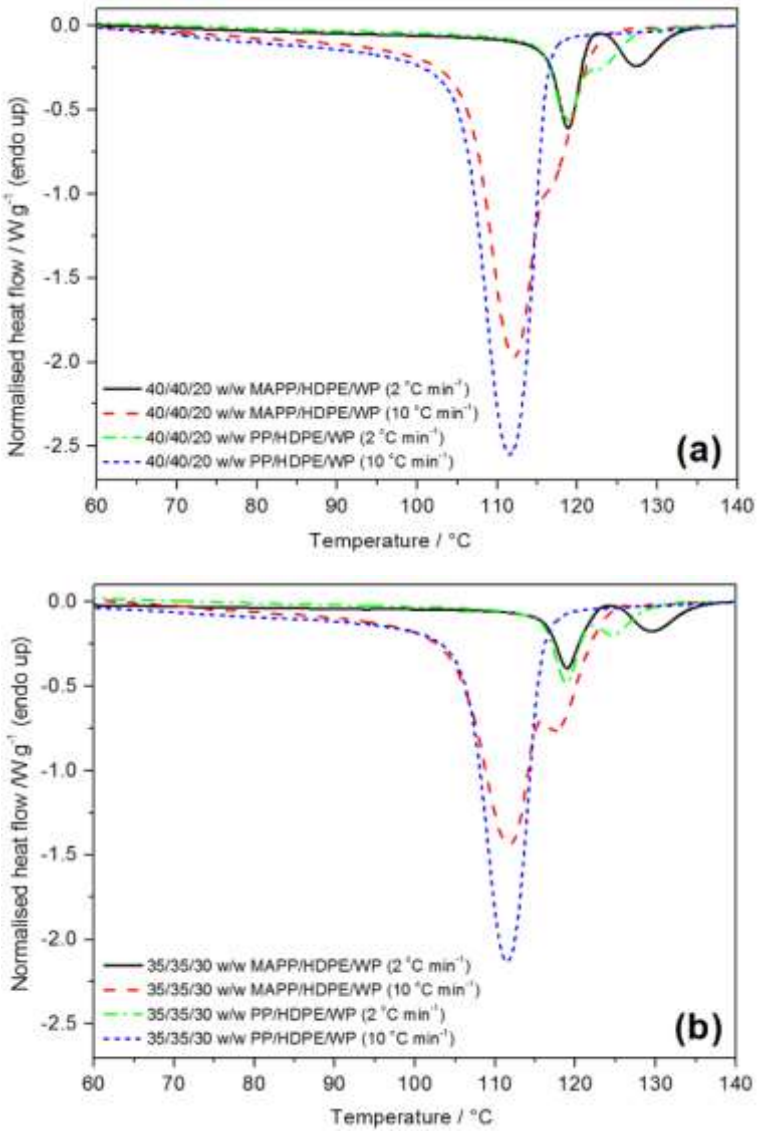

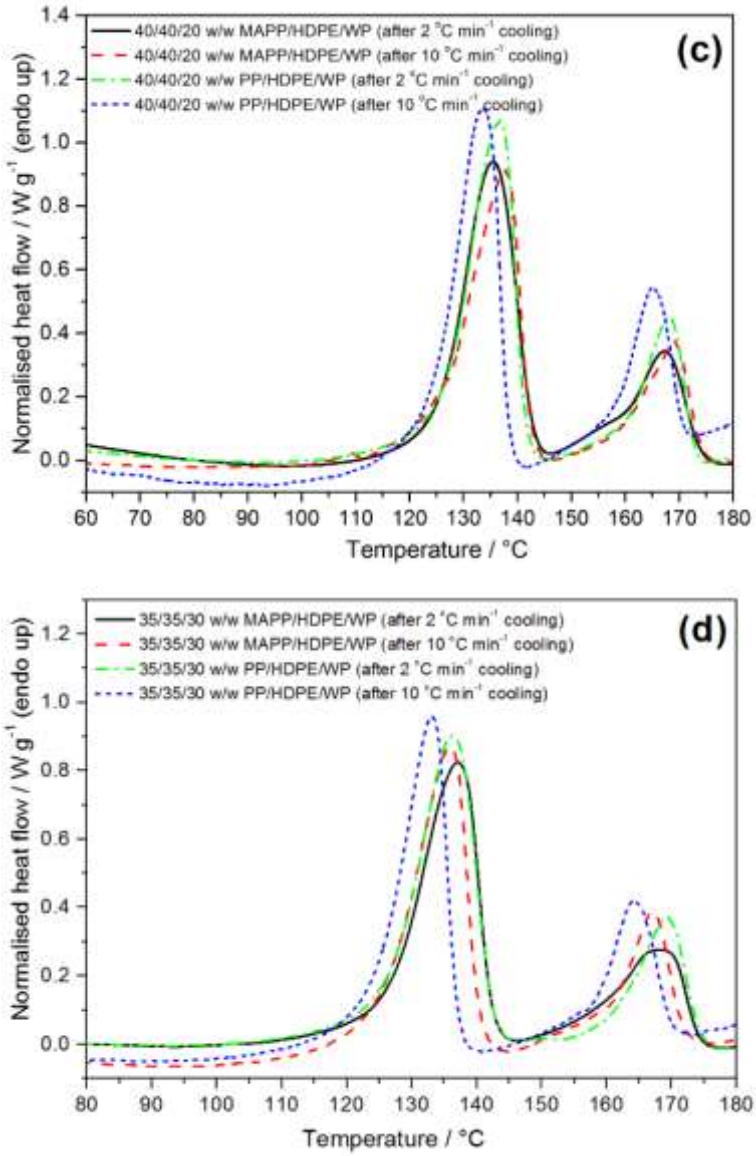

Figure 6 DSC (a,b) cooling and (c,d) heating curves of the blend composites

The second observation is that, in the case of PP/HDPE/WP, (i) the T_m of PP increases with increasing WP content, but only for the 2 °C min^{-1} cooled samples, and (ii) the χ_c of PP decreases with increasing WP content, but only for the 10 °C min^{-1} cooled samples. The first observation may be explained through the formation of larger PP crystallites through its interaction with the WP particles during the slower cooling. During the faster cooling there was obviously not enough time for the crystallites, formed on the surfaces of the WP particles, to grow into larger crystallites. The decrease in total PP crystallinity with increasing WP content during faster cooling may be linked to a combination of transcrystallization of the PP on the WP surfaces and co-crystallization of the shorter PP chains with HDPE.

The third observation is that, in the case of MAPP/HDPE/WP, (i) the χ_c of HDPE decreases with increasing WP content, but only for the 2 °C min^{-1} cooled samples, (ii) the T_m of MAPP increases with increasing WP content after both cooling rates, (iii) the T_c of MAPP increases with increasing WP content, but only during 2 °C min^{-1} cooling, and (iv) the χ_c of MAPP decreases with increasing WP content, but only after 10 °C min^{-1} cooling. All these observations may be linked to the fact that the WP particles, that act as nucleation centres for MAPP crystallization, interact fairly strongly with MAPP because of the functional groups on the WP surfaces and on the MAPP chains. The MAPP probably grows into fairly large spherulites on the surfaces of the WP particles, even at a cooling rate of 10 °C min^{-1}, and these larger spherulites give rise to melting at higher temperatures. Since MAPP crystallizes fairly slowly, the nucleation by the WP particles seems to be more effective at the slower cooling rate, and therefore the T_c only increased when the sample was cooled at 2 °C min^{-1}. The reason for the decrease in MAPP crystallinity with increasing WP content after cooling at 10 °C min^{-1} is not entirely clear, but it may be that the interaction between WP and MAPP to some extent immobilized the MAPP chains and prevented its effective crystallization at the faster cooling rate.

The last observation is that cooling at 10 °C min^{-1} shows the existence of two peaks only for MAPP/HDPE/WP. The peaks are also more resolved at the higher WP content. Again the reason is the stronger interaction of WP with MAPP which results in the MAPP starting to crystallize at higher temperatures, even during faster cooling.

3.4 Tensile testing

The tensile results for all the samples are summarized in Figure 7 and Table 3. HDPE was found to have the highest Young's modulus (E) of 881 MPa, while PP and MAPP had moduli of 500 and 378 MPa, respectively. The PP/HDPE and MAPP/HDPE blends had higher Young's moduli than the two neat polymers that made up the blend (Figure 6(a)), similar to findings by other authors [33,44]. It has been reported that co-continuous blends have high Young's modulus values [45], which are the result of more effective stress transfer between the two polymers in the blends. According to these authors both phases contribute to the blend modulus in all directions. Since we mixed equal amounts of polymers in both types of blend, we can confidently assume that both had co-continuous morphologies, which would then give rise to higher tensile modulus values. The higher tensile modulus could be explained through

the nucleation of HDPE crystallization on the surfaces of already crystallized PP or MAPP, so that the interfaces between the two co-continuous polymers will have a higher crystallinity giving rise to more effective stress transfer between these polymers. The MAPP/HDPE blend had a higher modulus than the PP/HDPE blend, probably due to a stronger Van der Waals interaction between MAPP and HDPE, which reduced the chain mobility in this blend.

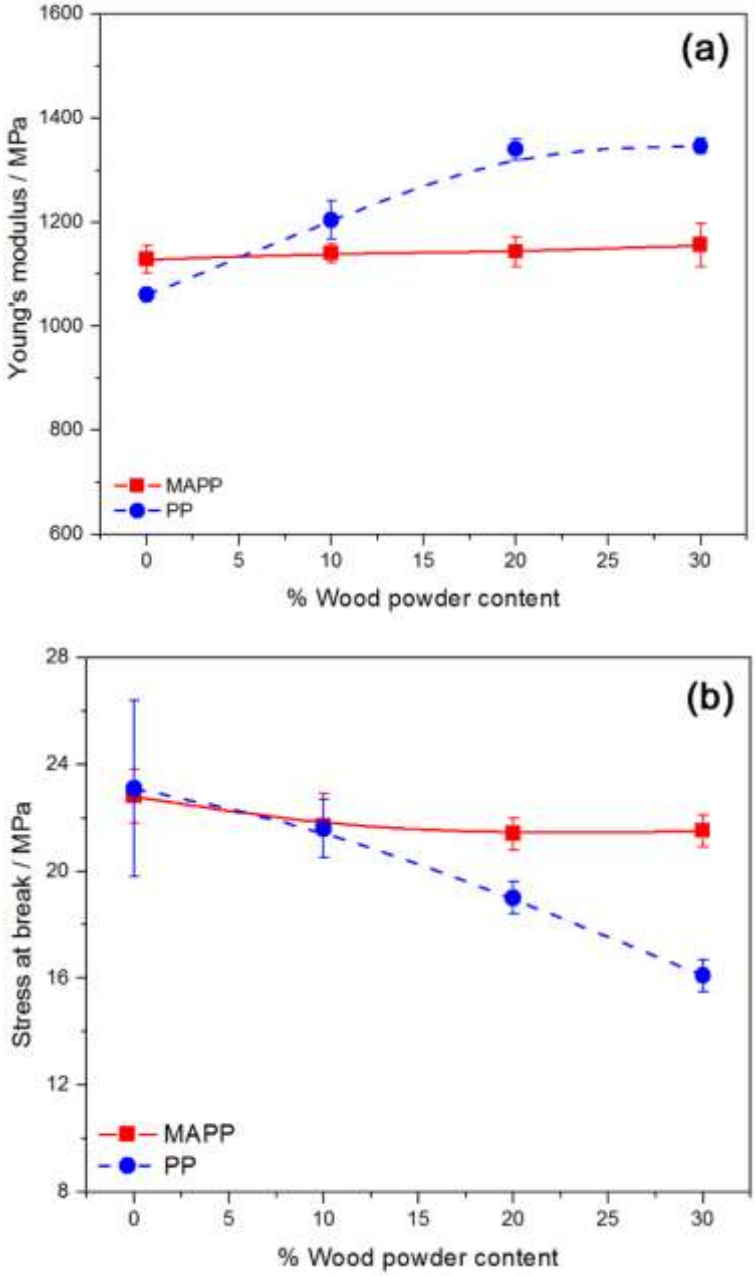

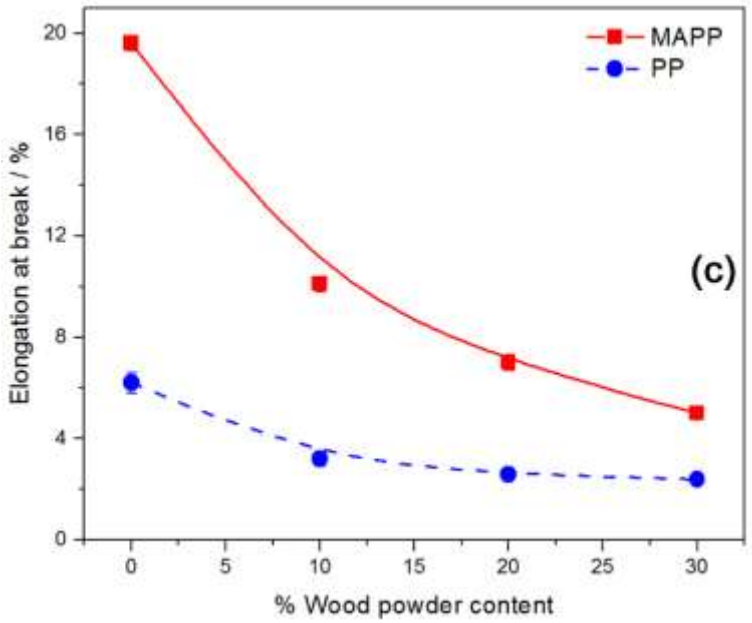

Figure 7 Tensile properties as function of WP content for all the investigated samples

Table 1 DSC melting data of the PP/HDPE system at two different cooling rates

HDPE peak →	**T_m / °C**		**ΔH_m^{exp} / J g^{-1}**		**χ_c / %**		**T_c / °C**	
PP/HDPE/WP (w/w)	**10 °C/min**	**2 °C/ min**	**10 °C/min**	**2 °C/ min**	**10 °C/min**	**2 °C/ min**	**10 °C/min**	**2 °C/ min**
Neat HDPE	136.3 ± 3.6	141.2 ± 2.8	218.8 ± 3.5	194.2 ± 2.1	75.8	67.2	112.7	118.7
50/50/0	134.7 ± 3.2	136.0 ± 1.9	100.9 ± 2.7	90.0 ± 0.8	69.9	62.3	111.2	118.1
45/45/10	134.5 ± 2.9	136.2 ± 1.7	87.7 ± 1.9	81.3 ± 1.1	67.5	69.2	111.9	118.2
40/40/20	133.7 ± 3.3	136.7 ± 2.0	78.6 ± 2.1	72.8 ± 1.5	68.0	69.2	111.6	118.5
35/35/30	133.5 ± 2.7	136.2 ± 2.3	67.1 ± 1.7	62.2 ± 1.3	66.4	68.1	111.5	118.6
PP peak →	**T_m / °C**		**ΔH_m^{exp} / J g^{-1}**		**χ_c / %**		**T_c / °C**	
PP/HDPE/WP (w/w)	**10 °C/min**	**2 °C/ min**	**10 °C/min**	**2 °C/ min**	**10 °C/min**	**2 °C/ min**	**10 °C/min**	**2 °C/ min**
Neat PP	164.8 ± 4.1	165.4 ± 2.1	79.3 ± 3.8	82.3 ± 1.9	37.9	39.4	110.8	121.4
50/50/0	165.9 ± 2.3	166.5 ± 2.9	25.8 ± 0.9	33.4 ± 0.6	24.7	32.0	111.2	118.1
45/45/10	165.7 ± 1.8	167.2 ± 3.4	19.6 ± 1.3	31.8 ± 0.4	20.8	33.8	111.9	120.2
40/40/20	165.4 ± 3.4	168.2 ± 1.9	17.4 ± 0.7	28.9 ± 0.7	20.8	34.6	111.6	123.5
35/35/30	164.7 ± 2.1	169.2 ± 2.0	13.5 ± 0.5	24.6 ± 0.5	18.5	33.6	111.5	124.7

T_m – melting peak temperature; ΔH_m^{exp} – experimentally observed melting enthalpy; T_c-crystallization temperature; χ_c – degree of crystallinity

Table 2 DSC melting data of the MAPP/HDPE system at two different cooling rates

HDPE peak →	**T_m / °C**		**ΔH_m^{exp} / J g^{-1}**		**χ_c / %**		**T_c / %**	
MAPP/HDPE/WP (w/w)	**10 °C/min**	**2 °C/ min**	**10 °C/min**	**2 °C/min**	**10 °C/min**	**2 °C/min**	**10 °C/min**	**2 °C/min**
Neat HDPE	136.3 ± 3.6	141.2 ± 2.8	218.8 ± 3.5	194.2 ± 3.0	75.8	67.2	112.7	118.7
50/50/0	134.9 ± 2.4	136.7 ± 1.8	97.3 ± 1.6	90.1 ± 1.3	67.5	62.4	113.7	120.7
45/45/10	136.6 ± 1.8	135.9 ± 2.4	81.9 ± 2.7	72.9 ± 1.1	63.0	56.1	111.2	119.4
40/40/20	137.2 ± 3.1	136.9 ± 2.6	75.1± 1.9	66.9 ± 2.3	65.0	57.9	111.7	119.4
35/35/30	136.6 ± 2.2	137.2 ± 2.8	64.6 ± 2.1	54.6 ± 1.7	63.9	54.0	111.5	119.0
MAPP peak →	**T_m / °C**		**ΔH_m^{exp} / J g^{-1}**		**χ_c / %**		**T_c / %**	
MAPP/HDPE/WP (w/w)	**10 °C/min**	**2 °C/ min**	**10 °C/min**	**2 °C/ min**	**10 °C/min**	**2 °C/ min**	**10 °C/min**	**2 °C/ min**
Neat MAPP	161.8 ± 4.1	164.5 ± 1.9	75.3 ± 3.8	77.4 ± 0.9	36.0	37.0	110.0	119.7
50/50/0	165.7 ± 2.1	166.5 ± 2.6	27.5 ± 0.5	31.3 ± 0.6	26.3	29.9	113.7	120.7
45/45/10	167.0 ± 2.9	166.1 ± 1.1	22.3± 1.2	30.7 ± 1.2	23.7	32.6	111.2	126.7
40/40/20	167.5 ± 2.4	167.5 ± 2.3	20.2 ± 0.4	25.4 ± 0.7	24.1	30.4	111.7	127.3
35/35/30	168.3 ± 2.0	168.4 ± 2.9	16.2 ± 0.3	22.0 ± 0.8	22.1	30.1	111.8	129.6

T_m – melting peak temperature; ΔH_m^{exp} – experimentally observed melting enthalpy; T_c-crystallization temperature; χ_c – degree of crystallinity

The presence of WP and increase in WP content resulted in a continuous increase in Young's modulus of the PP/HDPE/WP composites, while that of the MAPP/HDPE/WP composites remained fairly constant. Wood and wood products have higher moduli than most polyolefins, and the incorporation of the WP is expected to increase the composite stiffness. This is, however, only observed in the PP/HDPE/WP composites. Arroyo *et al*. [44] studied the mechanical behaviour of polypropylene/polyethylene blends/organo-bentonite nanocomposites, and reported that the weaker the matrix, the stronger the reinforcing effect of the filler. In our case there seems to be a stronger interaction between MAPP and HDPE than between PP and HDPE, and the WP particles are primarily located in the MAPP phase, giving rise to a complicated interaction mechanism that may explain the fact that the presence of WP in MAPP/HDPE had little influence on the Young's moduli of these samples.

The tensile strengths of the three neat polymers have the same order of magnitude, but that of PP is somewhat higher than the others (Figure 7(b), Table 3)**.** Salih *et al*. [33] used the molecular structures of the pure polymers to explain the difference in the tensile strength. According to them PP has a higher strength and stiffness due to the orderly branch distribution that promotes PP crystallization and restricts chain rotation, producing a stronger but less flexible material. The introduction of maleic anhydride on the PP chain disturbs the order and leads to a weaker and less stiff material. The few branches in the HDPE structure allows the polymer chains to pack themselves closely together, so the intermolecular forces are stronger, resulting in a dense, highly crystalline material of moderate stiffness.

Table 3 Tensile properties of all the investigated samples

	E / MPa	**σ_b / MPa**	**ε_b / %**	**E / MPa**	**σ_b / MPa**	**ε_b / MPa**
w/w	**MAPP/HDPE/WP**			**PP/HDPE/WP**		
100/0/0	472 ± 15	24.9 ± 0.7	13.3 ± 1.2	499 ± 14	29.9 ± 1.3	14.7 ± 2.5
0/100/0	881 ± 37	22.4 ± 1.2	21.9 ± 0.2	881 ± 37	22.4 ± 1.2	21.9 ± 0.2
50/50/0	1128 ± 26	22.8 ± 0.9	19.6 ± 0.3	1060 ± 1	23.1 ± 3.3	6.2 ± 0.4
45/45/10	1140 ± 18	21.7 ± 1.2	10.1 ± 0.3	1204 ± 37	21.6 ± 1.1	3.2 ± 0.3
40/40/20	1143 ± 28	21.4 ± 0.6	7.0 ± 0.3	1340 ± 20	19.0 ± 0.6	2.6 ± 0.2
35/35/30	1156 ± 41	21.5 ± 0.6	5.0 ± 0.1	1346 ± 15	16.1 ± 0.6	2.4 ± 0.2

E – tensile modulus, σ_b – tensile strength at break, ε_b – elongation at break

The tensile strengths of the PP/HDPE and MAPP/HDPE blends are within the same order of magnitude as those of the two individual polymers (Table 3, Figure 7(b)). Table 3 shows that the tensile strengths of HDPE, PP and MAPP are almost the same within

experimental error. According to the law of averages one would not expect any change in the tensile strengths of the blends. Lin *et al*. [1] prepared and evaluated the compatibility of a 75/25 w/w PP/HDPE polyblend. They also reported similar tensile strengths for the individual polymers and the blend.

Fillers often decrease the tensile strength of materials; exceptions result when the filler is extremely fine or when there is an interaction between the filler and the polymer matrix [33]. In our case, the filler had a negative effect on the tensile strength of the PP/HDPE blend (Figure 7(b)), while the tensile strength of MAPP/HDPE/WP remained fairly constant with an increase in the filler content. PP and HDPE in the PP/HDPE blend are incompatible and the WP filler particles acted as defect centres for the initiation of cracks, which then easily propagated along the interfaces between the two polymers. In the case of the MAPP/HDPE/WP composites, the WP interacted with the anhydride functionality in MAPP, resulting in good stress transfer between WP and MAPP. Crazes probably formed at the WP surfaces, but because all the WP particles were restricted to the MAPP phase, these crazes probably terminated at neighbouring WP particles and did not develop into cracks that would propagate along the interfaces between MAPP and HDPE.

The elongation at break of HDPE was significantly larger than those of PP and MAPP, while these two polymers had almost the same elongation at break values (Figure 7(c), Table 3). Salih *et al*. [33] studied PP/HDPE blends and reported that HDPE showed elastic behaviour, giving a larger elongation at break than PP. The MAPP/HDPE blend had a significantly larger elongation at break than the PP/HDPE blend for the same reason discussed in the previous paragraph.

A continuous decrease in elongation at break was observed with increasing WP content for both the blends (Figure 7(c)). The rigid particulate WP filler particles acted as defect centres for the initiation and propagation of cracks in both composites. However, the MAPP/HDPE/WP composites have larger elongation at break values than the PP/HDPE/WP composites. The reason is the stronger interaction between MAPP and WP which opposed crack propagation through the MAPP-WP interfaces and gave rise to longer elongations before fracture.

3.5 Thermogravimetric analysis (TGA)

The TGA and derivative TGA (DTG) curves of the investigated samples are shown in Figure 8, and the respective temperatures are summarized in Table 4. All the neat polymers and the

MAPP/HDPE blend show a single degradation step, but not the PP/HDPE blend (Figure 8(b)). The first step for PP/HDPE corresponds to the degradation of the neat PP, and can therefore be associated with the degradation of the PP phase of the blend. The second degradation is related to the degradation of the neat HDPE, and can be associated with the degradation of the HDPE component in the blend. This is further confirmation of the immiscibility of the two polymers in this blend. This is not observed for the MAPP/HDPE blend, probably due to a stronger interaction between these two polymers. The thermal stability of the polymers and the blends followed the order: PP/HDPE < MAPP/HDPE < PP < MAPP < HDPE. At 500 °C the neat polymers and the two polymer blends were completely decomposed (Figure 8(a)). The PP/HDPE blend was less thermally stable than the MAPP/HDPE blend because PP was less thermally stable than MAPP.

Cellulosic substances normally have three degradation steps. Depolymerisation of hemicelluloses takes place between 150 and 350 °C, random cleavage of glycosidic linkages of cellulose occurs between 280 and 350 °C, and the degradation of lignin occurs between 250 and 500 °C [46-48]. The DTG curve for WP in Figure 8(b) shows an overlap of two weight loss processes, which is probably the depolymerisation of hemicelluloses and the random cleavage of glycosidic linkages of cellulose, followed by the degradation of lignin. The two blend composites show two degradation steps. The first step corresponds to the degradation of WP. Degradation products, such as volatile carbon monoxide and methane, and char residue are formed. The second step corresponds to the degradation of the polymer blend matrix. The incorporation of WP into the two blends leads to an increase in the temperature of the second degradation step compared to the neat blends. The char residue, formed during the degradation of WP, probably delayed the heat transfer to the polymer blend matrix, and acted as a barrier which slowed down the escape of the volatile products formed during the matrix degradation process. It is further obvious that the degradation of WP in the blend composites shifted to higher temperatures, which is something one would expect because of the thermal protection provided by the surrounding polymer.

Table 4 DTG peak temperatures of all the investigated samples

Sample (w/w)	MAPP/HDPE/WP		PP/HDPE/PP	
	Peak 1 / °C	Peak 2 / °C	Peak 1 / °C	Peak 2 / °C
100/0/0	465	-	458	-
0/100/0	486	-	486	-
50/50/0	455	-	406	445
45/45/10	453	-	455	-
40/40/20	374	455	374	455
35/35/30	374	475	378	455 and 485

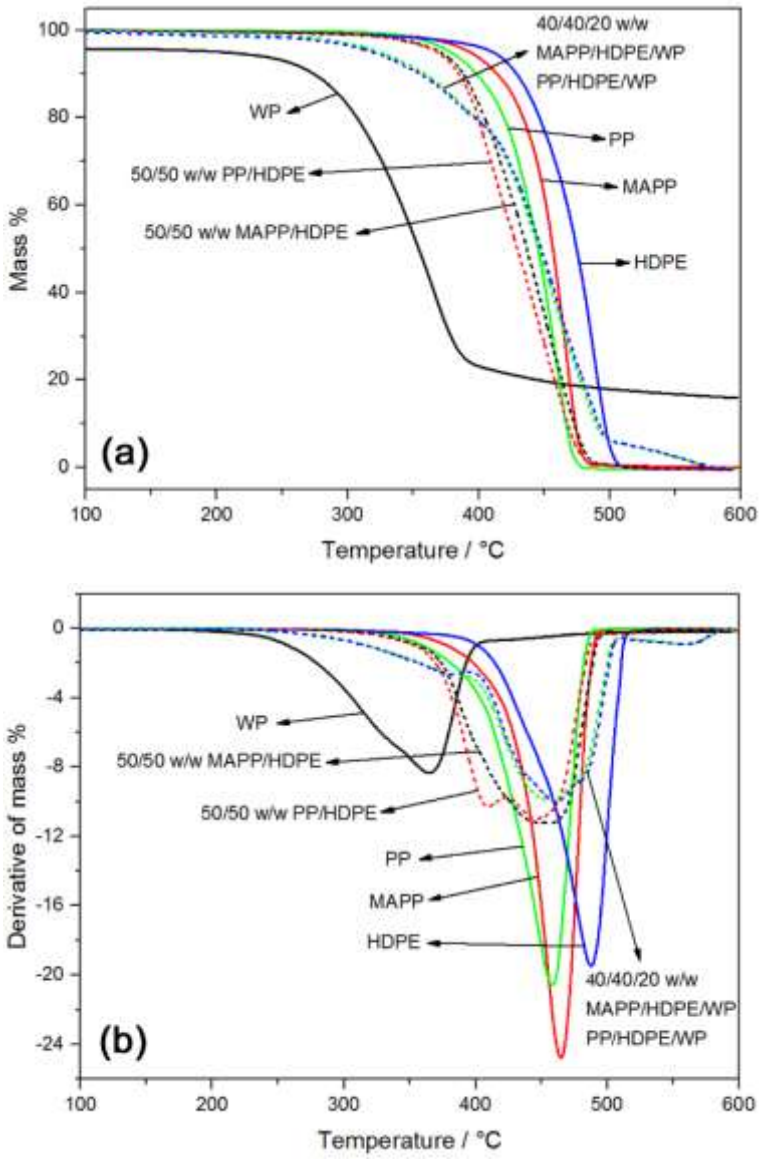

Figure 8 (a) TGA and (b) DTG curves of the neat polymers, the blends, and selected composites

4. Conclusions

The PP/HDPE and MAPP/HDPE blends showed two-phase morphologies, but there were indications of a better interaction between MAPP and HDPE than between PP and HDPE. The WP clearly interacted strongly with the MAPP through the formation of hydrogen bonds between the functional groups. The melting peaks show a clear distinction between PP, MAPP and HDPE, but each of the blends showed one crystallization peak. This was a clear indication of the faster crystallization of the more linear HDPE chains. MAPP and HDPE showed separate crystallization peaks in the MAPP/HDPE/WP composites, and this separation of the crystallization became more resolved with increasing WP content and at lower cooling rates. Even PP started crystallizing separately in the PP/HDPE/WP composites at high WP contents and low cooling rates, indicating some interaction between PP and WP. The Young's modulus increased and the stress at break decreased with increasing WP content, and these effects were more pronounced in the PP/HDPE/WP composites, probably because of the stronger interaction between MAPP and WP. Although the elongation at break decreased with increasing WP content for both types of composite, these values were significantly higher for the MAPP/HDPE/WP composites. The presence of WP increased the thermal stability of both the MAPP/HDPE and PP/HDPE matrices, probably because the char from the WP decomposition acted as a barrier which delayed the heat transfer to the polymer matrices.

Compliance with ethical standards:

Funding: There was no specific funding for this study.

Conflict of interest: The authors declare that they have no conflict of interest.

References

1. J.H. Lin, Y.J. Pan, C.F. Liu, C.L. Huang, C.T. Hsieh, C.K. Chen, Z.I. Lin, C.W. Lou. Preparation and compatibility evaluation of polypropylene/high density polyethylene polyblends. Materials 2015; 8:8850-8859.
   DOI: 10.3390/ma8125496
2. W. Camacho, S. Karlson. Assessment of thermal and thermo-oxidative stability of multi-extruded recycled PP, HDPE and a blend thereof. Polymer Degradation and Stability 2002; 78:385-391.

DOI: 10.1016/S0141-3910(02)00192-1

3. A.M.C. Souza, N.R. Demarquette. Influence of composition on the linear viscoelastic behavior and morphology of PP/HDPE blends. Polymer 2002; 43:1313-1321.
   DOI: 10.1016/S0032-3861(01)00718-2
4. A.M.C. Souza, N.R. Demarquette. Influence of coalescence and interfacial tension on the morphology of PP/HDPE compatibilized blends. Polymer 2002; 43:3959-3967.
   DOI: 10.1016/S0032-3861(02)00223-9
5. S. Jose, A.S. Aprem, B. Francis, M.C. Chandy, P. Werner, V. Alstaedt, S. Thomas. Phase morphology, crystallisation behaviour and mechanical properties of isotactic polypropylene/high density polyethylene blends. European Polymer Journal 2004; 40:2105-2115.
   DOI: 10.1016/j.eurpolymj.2004.02.026
6. H.P. Blom, J.W. Teh, A. Rudin. i-PP/HDPE blends. III. Characterization and compatibilization at lower i-PP contents. Journal of Applied Polymer Science 1996; 61:959-968.
   DOI**:** 10.1002/ (SICI) 1097-4628(19960808)61:6<959:AID-APP10>3.0.CO;2-Q
7. A.H.I. Mourad. Thermo-mechanical characteristics of thermal aged polyethylene/ polypropylene blends. Materials and Design 2010; 31:918-929.
   DOI: 10.1016/jmatdes.2009.07.031
8. S.A. Ramazani, M.A. Valami, M. Khak. Effect of poly(propylene-g-maleic anhydride) on the morphological, rheological, and mechanical properties of PP/HDPE blend. Journal of Thermoplastic Composite Materials 2009; 22:519-530.
   DOI: 10.1177/0892705709100662
9. Z. Bartczak, A.S. Argona, R.E. Cohena, M. Weinberg. Toughness mechanism in semi-crystalline polymer blends: II. High-density polyethylene toughened with calcium carbonate filler particles. Polymer 1999; 40:2347-2365.
   DOI: 10.1016/S0032-3861(98)00444-3
10. B.A. Acha, N.E. Marcovich, M.M. Reboredo. Lignin in jute fabric-polypropylene composites. Journal of Applied Polymer Science 2009; 113:1480-1487.
    DOI: 10.1002/app.29999
11. M. Canetti, F. Bertini, A. De Chirico, G. Audisio. Thermal degradation behaviour of isotactic polypropylene blended with lignin. Polymer Degradation and Stability 2006; 91:494-498.
    DOI: 10.1016/j.polymdegradstab.2005.01.052

12. J.G. Gwon, S.Y. Lee, S.J. Chun, G.H. Doh, J.H. Kim. Effect of chemical treatments of wood fibers on the physical strength of polypropylene based composites. Korean Journal of Chemical Engineering 2010; 27:651-657.
DOI: 10.1007/s11814-010-0058-1
13. H.S. Kim, B.H. Lee, S.W. Choi, S. Kim, H.J. Kim. The effect of types of maleic anhydride-grafted polypropylene (MAPP) on the interfacial adhesion properties of bio-flour-filled polypropylene composites. Composites Part A 2007; 38:1473-1482.
DOI: 10.1016/j.compositesa.2007.01.004
14. X. Zhou, Y. Yu. Q. Lin, L. Chen. Effect of maleic anhydride polypropylene (MAPP) on the physico-mechanical properties and rheological behaviour of bamboo powder-propylene foamed composites. BioResources 2013; 8:6263-6279.
15. F.C. Chiu, H.Z. Yen, C.E. Lee. Characterization of PP/HDPE blend-based nanocomposites using different maleated polyolefins as compatibilizers. Polymer Testing 2010; 29:397-406.
DOI: 10.1016/j.polymertesting.2010.01.004
16. F.C. Chiu, H.Z. Yen, C.C. Chen. Phase morphology and physical properties of PP/HDPE/organoclay (nano) composites with and without a maleated EPDM as a compatibilizer. Polymer Testing 2010; 29:706-716.
DOI: 10.1016/j.polymertesting.2010.05.013
17. L. Cao, S. Deng, Z. Lin. Enhancement of carbon nanotube particle distribution in PPS/PEEK/carbon nanotube ternary composites with sausage-like structure. Polymers 2016; 8:50.
DOI: 10.3390/polym8020050
18. C.I.W. Calcagno, C.M. Mariani, S.R. Teixeira, R.S. Mauler. The role of the MMT on the morphology and mechanical properties of the PP/PET blends. Composites Science and Technology 2008; 68:2193-2200.
DOI: 10.1016/j.compscitech.2008.03.012
19. K.M. Seven, M.C. Jeffrey, J.F. Gilchrist. Nucleating agents for high-density polyethylene - A review. Polymer Engineering and Science 2016; 58:541-554.
DOI: 10.1002/pen.24278
20. E. Zhuravlev, V. Madhavi, A. Lustiger, R. Androsch, C. Schick. Crystallization of polyethylene at large undercooling. ACS Macro Letters 2016; 5:365-370.
DOI: 10.1021/acsmacrolett.5b00889
21. S.L. Kodjie, L. Li, B. Li, W. Cai, C.Y. Li, M. Keating. Morphology and crystallization behavior of HDPE/CNT nanocomposite. Journal of Macromolecular Science, Part B: Physics 2006; 45:231-245.

DOI: 10.1080/00222340500522299

22. A.R. Bhattacharyya, T.V. Sreekumar, T. Liu, S. Kumar, L.M. Ericson, R.H. Hauge, E. Smalley. Crystallization and orientation studies in polypropylene/single wall carbon nanotube composite. Polymer 2003; 44:2373-2377.
DOI: 10.1016/S0032-3861(03)00073-9

23. T.P Mohan, K. Kanny. Melt blend studies of nanoclay-filled polypropylene (PP)-high-density polyethylene (HDPE) composites. Journal of Materials Science 2013; 48: 8292-8301.
DOI: 10.1007/s10853-013-7642-9

24. Y. Lei, Q. Wu, C.M. Clemons, F. Yao, Y. Xu. Influence of nanoclay on properties of HDPE/wood composites. Journal of Applied Polymer Science 2007; 106:3958-3966.
DOI: 10.1002/app.27048

25. Y.H. Cui, J. Tao, B. Noruziaan, M. Cheung, S. Lee. DSC analysis and mechanical properties of wood–plastic composites. Journal of Reinforced Plastics and Composites 2010; 29:278-289.
DOI: 10.1177/0731684408097766

26. C. Zhang, X.S. Yi, S. Asai, M. Sumita. Morphology, crystallization and melting behaviors of isotactic polypropylene/high density polyethylene blend: Effect of the addition of short carbon fiber. Journal of Materials Science 2000; 35:673-683.
DOI: 10.1023/A:1004749015907

27. G. Keledi, A. Sudár, C. Burgstaller, K. Renner, J. Móczó, B. Pukánszky. Tensile and impact properties of three-component PP/wood/elastomer composites. eXPRESS Polymer Letters 2012; 6:224-236.
DOI: 10.3144/expresspolymlett.2012.25

28. H. Gao, Y.M. Song, Q.W. Wang, Z. Han M.L. Zhang. Rheological and mechanical properties of wood fiber-PP/PE blend composites. Journal of Forestry Research 2008; 19:315-318.
DOI: 10.1007/s11676-008-0057-9

29. A. Grisa, M. Zeni. Structural analysis of (LDPE) and (HDPE) films biodegraded in sanitary landfill-II. Macromolecular Symposia 2006; 245:607-610.
DOI: 10.1002/masy.200651387

30. D.G. Dikobe, A.S. Luyt. Comparative study of the morphology and properties of PP/LLDPE/wood powder and MAPP/LLDPE/wood powder polymer blend composites. eXPRESS Polymer Letters 2010; 4:729-741.
DOI: 10.3144/expresspolymlett.2010.88

31. B. Na, K. Wang, Q. Zhang, R. Du, Q. Fu. Tensile properties in the oriented blends of high-density polyethylene and isotactic polypropylene obtained by dynamic packing injection moulding. Polymer 2005; 46: 3190-3198.
DOI: 10.1016/j.polymer.2005.01.094

32. C. Clemmons. Elastomer modified polypropylene–polyethylene blends as matrices for wood flour–plastic composites. Composites Part A: Applied Science and Manufacturing 2010; 41: 1559-1569.
DOI: 10.1016/j.compositesa.2010.07.002

33. S.E. Salih, A.F. Hamood, A.H. Abdalsalam. Comparison of the characteristics of LDPE:PP and HDPE:PP polymer blends. Modern Applied Science 2013; 7:33-42.
DOI: 10.5539/mas.v7n3p33

34. C. Tselios, D. Bikiaris, V. Maslis, C. Panayiotou. In situ compatibilization of polypropylene polyethylene blends: A thermomechanical and spectroscopic study. Polymer 1998; 39:6807-6817.
DOI: 10.1016/S0032-3861(98)00132-3

35. J.V. Gulmine, P.R. Janissek, H.M. Heise, L. Akecelrud. Polyethylene characterisation by FTIR. Polymer Testing 2002; 21:557-563.
DOI: S0142-9418(01)00124-6

36. M. Sclavons, M. Laurent, J. Devaux, V. Carlier. Maleic anhydride grafted polypropylene. FTIR study model grafted by ene-reaction. Polymer 2005; 46:8062-8067.
DOI: 10.1016/j.polymer.2005.06.115

37. W. Camacho, S. Karlsson. NIR, DSC, and FTIR as quantitative methods for compositional analysis of blends of polymers obtained from recycled mixed plastic waste. Polymer Engineering and Science 2001; 41:1626-1635.
DOI: 10.1002/pen.10860

38. A. Awal, S.B. Ghosh, M. Sain. Thermal properties and spectral characterization of wood pulp reinforced bio-composite fibers. Journal of Thermal Analysis and Calorimetry 2010; 99:695-701.
DOI: 10.1007/s10973-009-0100-x

39. J. Lisperguer, C. Nunez, P. Perez-Guerrero. Structure and thermal properties of maleated lignin-recycled polystyrene composites. Journal of the Chilean Chemical Society 2013; 58:1937-1940.
DOI: 10.4067/S0717-97072013000400005

40. L.J. Konwar, P. Mäki-Arvela, A.J. Thakur, N. Kumar, J.P. Mikkola. Sulfonated carbon as a new, reusable heterogeneous catalyst for one-pot synthesis of acetone soluble cellulose acetate. Royal Society of Chemistry Advances 2016; 6:8829-8837.
DOI: 10.1039/C5RA25716F
41. D. Ndiaye, L.M. Matuana, S. Morlat-Therias, L. Vidal, A. Tidjani, J.L. Gardette. Thermal and mechanical properties of polypropylene/wood-flour composites. Journal of applied polymer science 2011; 119:3321-3328.
42. A.S. Luyt, M.D. Dramićanin, Ž. Antić, V. Djoković. Morphology, mechanical and thermal properties of composites of polypropylene and nanostructured wollastonite filler. Polymer Testing 2009; 28:348-356.
DOI: 10.1016/j.polymertesting.2009.01.010
43. J. Finlay, S. Sheppard, S. Tookey, M.J. Hill, P.J. Barham. Unexpectedly high Young's moduli recorded for iPP/HDPE blends. Journal of Polymer Science Part B: Polymer Physics 2001; 39:1404-1414.
DOI: 10.1002/polb.1112
44. M. Arroyo, R.V. Suarez, B. Herrero, M.A. Lopez-Manchado. Optimisation of nanocomposites based on polypropylene/polyethylene blends and organo-bentonite. Journal of Materials Chemistry 2003; 13:2915-2921.
DOI: 10.1039/b306108f
45. H.G.B. Premalal, H. Ismail, A. Baharin. Comparison of the mechanical properties of rice husk powder filled polypropylene composites with talc filled polypropylene composites. Polymer Testing 2002; 21:833-839.
DOI: 10.1016/S0142-9418(02)00018-1
46. Y.M. Krivoguz, S.S. Pesetskii, B. Jurkowski, T. Tomczyk. Structure and properties of polypropylene/low-density polyethylene blends grafted with itaconic acid in the course of reactive extrusion. Journal of Applied Polymer Science 2006; 102:1746-1754.
DOI: 10.1002/app.23998
47. N.V. Penava, V. Rek, I.F. Houra. Effect of EPDM as a compatibilizer on mechanical properties and morphology of PP/LDPE blends. Journal of Elastomers and Plastics 2012; 45:391-403.
DOI: 10.1177/0095244312457162
48. H.S. Kim, H.S. Yang, H.J. Kim, H.J. Park. Thermogravimetric analysis of rice husk flour filled thermoplastic polymer composites. Journal of Thermal Analysis and Calorimetry 2004; 76:395-404.
DOI: 10.1023/B:JTAN.0000028020.02657.9b